NANO LETTERS

LETTER

pubs.acs.org/NanoLett

Are Nanoporous Materials Radiation Resistant?

E. M. Bringa,[†] J. D. Monk,[‡] A. Caro,[*,§] A. Misra,[§] L. Zepeda-Ruiz,[∥] M. Duchaineau,[∥] F. Abraham,[∥] M. Nastasi,[§] S. T. Picraux,[§] Y. Q. Wang,[§] and D. Farkas[⊥]

[†]CONICET & Instituto de Ciencias Básicas, Universidad Nacional de Cuyo, 5500 Mendoza, Argentina

[‡]Cain Department of Chemical Engineering, Louisiana State University, Baton Rouge, Louisiana 70803, United States

[§]Los Alamos National Laboratory, Los Alamos, New Mexico 97500, United States

[∥]Lawrence Livermore National Laboratory, Livermore, California 94551, United States

[⊥]Department of Materials Sciences, Virginia Tech, Blacksburg, Virginia 24061, United States

ABSTRACT:

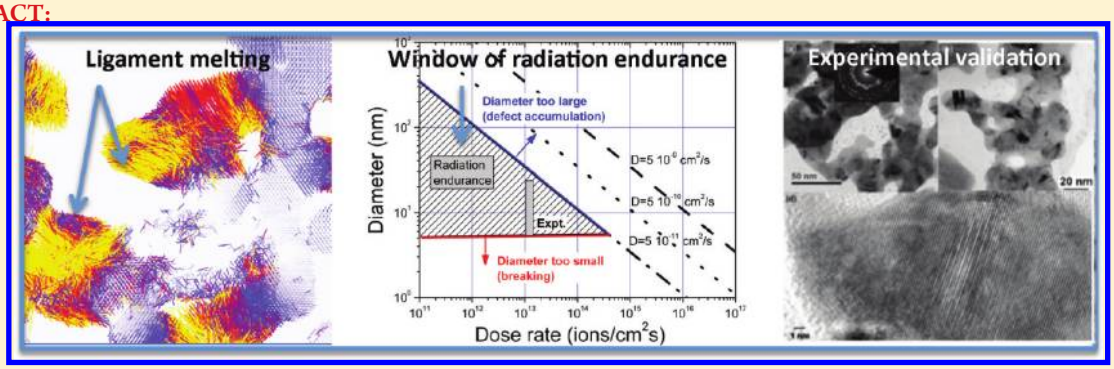

The key to perfect radiation endurance is perfect recovery. Since surfaces are perfect sinks for defects, a porous material with a high surface to volume ratio has the potential to be extremely radiation tolerant, provided it is morphologically stable in a radiation environment. Experiments and computer simulations on nanoscale gold foams reported here show the existence of a window in the parameter space where foams are radiation tolerant. We analyze these results in terms of a model for the irradiation response that quantitatively locates such window that appears to be the consequence of the combined effect of two length scales dependent on the irradiation conditions: (i) foams with ligament diameters below a minimum value display ligament melting and breaking, together with compaction increasing with dose (this value is typically ∼5 nm for primary knock on atoms (PKA) of ∼15 keV in Au), while (ii) foams with ligament diameters above a maximum value show bulk behavior, that is, damage accumulation (few hundred nanometers for the PKA's energy and dose rate used in this study). In between these dimensions, (i.e., ∼100 nm in Au), defect migration to the ligament surface happens faster than the time between cascades, ensuring radiation resistance for a given dose-rate. We conclude that foams can be tailored to become radiation tolerant.

KEYWORDS: Radiation damage, nanofoams, gold, computer simulations

Radiation damage is a factor determining the lifetime of numerous components of nuclear plants. Fuel, cladding, internals, and pressure vessel each suffer microstructural modifications that alter their properties as dose accumulates. Swelling, hardening, embrittlement, and creep are some of the most important properties that evolve with damage. New generations of fission and fusion reactors will require materials resistant to large levels of radiation without significant changes to their mechanical and thermal properties. Dense nanocrystals and nanocomposites have been proposed as possible candidates for such applications because grain and interphase boundaries act as point-defect sinks reducing damage accumulation and possible swelling.[1]

Radiation resistance is also important for the survival of spacecraft exposed to long-term or high dose-rate radiation exposure, as in the case of missions to Mars or the inner solar system.[2]

Different strategies are being explored to achieve radiation tolerance. In particular interfaces are believed to be one important feature to improve resistance to extreme conditions. Ferritic steels with improved properties are being developed via the addition of a large amount of interfaces between the matrix and nanoscale oxide precipitates; these are the oxide dispersion strengthened (ODS) steels that have proven to have swelling resistance well above 100 displacements per atom (dpa), and creep resistance above 600 °C.[1,3] Nanoscale metallic multilayers show extreme tolerance to He bubble swelling due to an enhancement of He solubility at particular types of face-centered cubic−body-centered cubic (fcc−bcc) interfaces.[4,5] Bulk nanocrystals can also display extraordinary radiation

Received: April 25, 2011
Revised: May 23, 2011
Published: June 09, 2011

healing behavior due to grain boundary accommodation of defects.[6,7]

Foams are materials with a large amount of interfaces (free surfaces in this case) with the potential to show radiation resistance due to the ideally unsaturable sink strength represented by free surfaces. In the case of nuclear fuels, which develop a natural foam-forming tendency due to fission gas accumulation, the idea of starting with a porous structure to accommodate the gas has been proposed for advanced fuels.[8] Nanocomposites, nanophase materials, and nanofoams could be unusually resistant to radiation because radiation-induced point defects cannot accumulate in the presence of the high density of defects sinks provided by interfaces and surfaces in these materials.

Because quasi one-dimensional materials such as nanofoams and nanowires both have a high-surface-area-per unit volume, they are ideal for the study of collision cascade effects when the structural dimension of a material is on the order of a typical collision cascade size. We found that this relation between cascade and ligament sizes is one of the two length scales that determine the overall behavior of foams under irradiation. The enhanced damage recovery is facilitated by the proximity of the surfaces that introduce image force effects, and by the local temperature increase in the region of the damage due to the much smaller quenching rate caused by dimensional effects, which enhances diffusion of the vacancies and interstitials well beyond bulk values.

Bulk nanocrystals and nanofoams represent distinct classes of materials with at least two fundamental differences regarding their radiation response: (i) the processes of thermalization of collision cascades in bulk nanocrystals is determined by the existence of surrounding material in all directions (3D cooling), a situation drastically different in nanofoams where ligamens are bounded by free surfaces that cannot transport heat away (1D cooling); and (ii) the properties of ligament surfaces in relation to their efficiency to trap and recombine defects are substantially different from the properties of the interfaces or grain boundaries in nanocrystalline solids: the presence of free surfaces create image forces that introduce a driving force enhancing defect migration, increasing the sink strength compared to interfaces in bulk materials. This enhanced diffusion sets the second relevant time/length scale we found for this problem, namely a characteristic time scale for defect annihilation related to ligament size. This time scale determines an upper dose-rate limit for radiation endurance, as we discuss below.

In this work, we study the effects of foam ligament sizes on the irradiation response, and from these results we propose the existence of a window in foam parameter space where foams are radiation tolerant. In addition to foams, we also examine the irradiation response of metallic nanowires, which are viewed as a unit segment of a foam ligament. Our results represent a contribution to the exploration of the fundamental aspects of irradiation response at exceedingly small length scales.

Simulation Results. There are relatively few atomistic simulations of solids with large porosity.[9−13] We generated foams using a methodology described in ref 10 with mean ligament size of 2−5 nm (density 43% of bulk value). Our simulations were carried out using LAMMPS [http://lamps.sandia.gov] and an EAM interatomic potential for Au.[14] After relaxation for 20 ps at 300 K and zero pressure, we introduced randomly chosen primary knock on atoms (PKAs) with 10−40 keV energy with its velocity in a random direction. This was repeated 10 times to simulate cumulative radiation damage at room temperature.

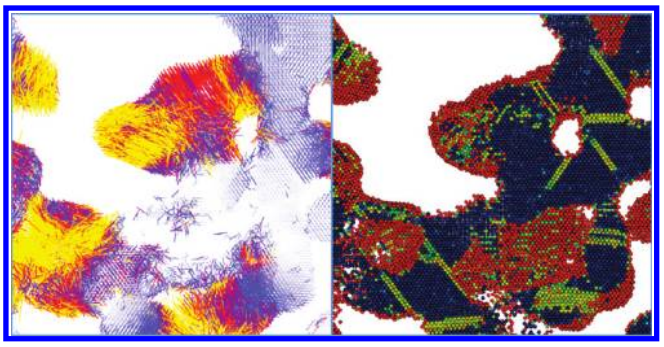

Figure 1. Irradiation of nanofoams, computer simulation. Small region of the sample with 45% porosity and a ∼5 nm ligament size, ∼110 ps after a cascade began, melted and recrystallized the tip of a ligament. (Left) Atomic displacements larger than the lattice parameter a_0 are shown with red indicating more than 4 a_0. (Right) Atoms colored by centro-symmetry parameter: blue indicates normal fcc material, green indicates SFs and twins, and red indicates highly disordered regions. Note the planar defects surrounding the void close to the cascade.

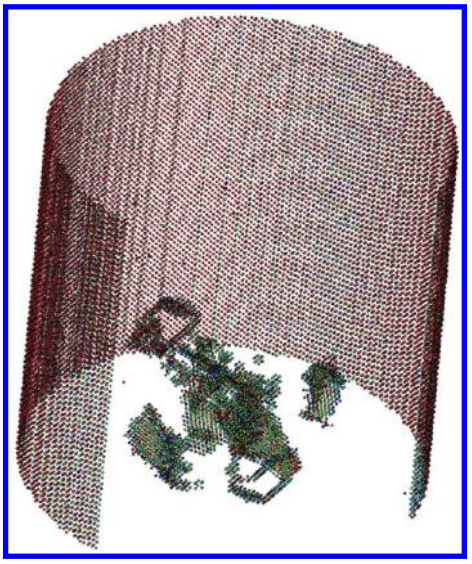

Figure 2. Response of an individual filament to irradiation. A 40 keV self-PKA at the center of a Au filament with D = 25 nm. Only defective atoms are shown 110 ps after the initial collision. The surface of the filament is also shown, except for a frontal cut to display the defects inside.

Our simulations show that cascades in Au foams with mean ligament size of up to a few nanometers lead to ligament break-up and compaction with dose. Figure 1 displays the atomic displacements in a sample ligament size of ∼5 nm induced by five PKAs of 40 keV. Note the large volume of influence of cascades. Experimental metallic nanofoams have ligament sizes ranging from 2 to tens of nanometers, the latter being many times the size of a dense collision cascade.[15−17] Simulation of foams with ligament sizes above ∼10 nm would be extremely expensive computationally; therefore we have simulated radiation damage in individual filaments of 15 and 25 nm diameters. We find no filament break-up and the formation of defect clusters collapsing into dislocation loops; we also observe migration of interstitials toward the surface with a few vacancy clusters migrating at a lower rate. For a PKA starting at its center, Figure 2 shows the

dx.doi.org/10.1021/nl201383u |Nano Lett. 2012, 12, 3351–3355

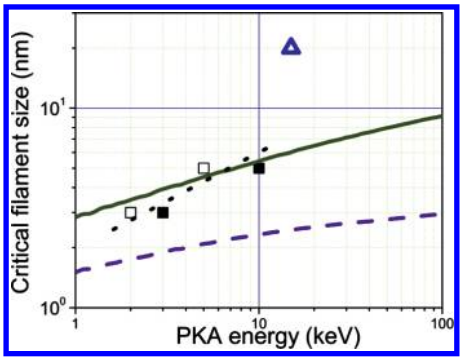

Figure 3. Lower critical size for radiation resistance. Solid line: linear size of a cascade versus PKA energy corresponding to Au projectile into Au target. Ligament sizes below this line would likely break. Squares: MD simulations for Au into Au filaments of two sizes. Open squares indicate runs where the filament breaks, while solid squares show filaments that do not break. Dashed line: size of a cascade versus PKA energy corresponding to Ne projectile into Au target. Similar to the Au projectile case, filament sizes below this line would likely break. Triangle: the point of the experimental irradiation of Ne into Au, clearly above the dashed line, that is, within the region of radiation endurance. Point line: guide to the eye for the critical size suggested by MD simulations.

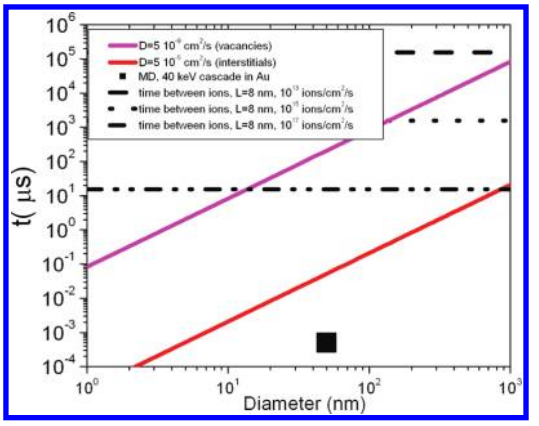

Figure 4. Upper critical size for radiation resistance. Time required for interstitials (lower solid line) and vacancies (upper solid line) to migrate to the surface of a ligament, estimated using parameters for migration of point defects in Au at room temperature. Broken lines: time between cascades within a cubic test volume of side $L = 8$ nm for three different dose-rates. Black square: MD result corresponding to migration of the interstitial clusters shown in Figure 2; it falls below the line corresponding to interstitials in the bulk instead of on top of it because diffusivity is enhanced by nearby surfaces. For a given irradiation dose-rate, a ligament does not accumulate damage if the diameter is less that the value where the vacancy solid line intersects the corresponding horizontal line. Diffusivities D for interstitials and vacancies are reported in the inset.

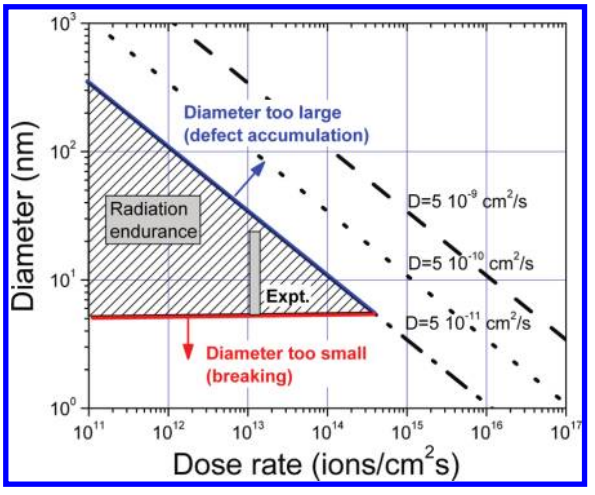

Figure 5. Window of radiation endurance. Map showing the window of radiation resistance (triangular area) in terms of the diameter of the foam ligaments and the dose-rate for the irradiation conditions explored in this work: 45 keV Ne ions into Au foam target at room temperature; radiation damage resistant ligaments are those with diameters above the lower critical size due to melting, extracted from Figure 3, and below the dose-rate line extracted from Figure 4. We show the upper critical limit for three different estimates of the diffusivities D of defect clusters, namely 5×10^{-9}, 5×10^{-10}, and 5×10^{-11} cm^2/sec.

defective atoms in the filament at the end of the collision cascade. On the basis of our MD results we then conclude that filament sizes below a lower critical size will be greatly affected by irradiation induced melting, while filaments above an upper critical size will behave as bulk materials.

To analyze the lower critical size, we construct a simple model by assuming that ligament breaking occurs when the size of the molten phase of the cascade equals the ligament size. We estimate the size of this molten volume by two means, namely, (i) assuming that most of the cascade energy is deposited within a cylinder with a length equal to the projected range plus the longitudinal straggling, and a radius equal to the radial straggling of the ion[18] (SRIM2000[19] has been used to obtain the ion range and straggling), and (ii) by a more elaborate method to calculate the volume of the melt as proposed by Alurralde et al. based on thermodynamic considerations.[20] Both methods give similar volumes differing by less than a factor of 2.

Figure 3 shows how the assumption of a critical breaking size for a given PKA energy (solid line for Au into Au irradiation) compares with results from molecular dynamics simulations of Au projectile into Au target (two filament sizes and two PKA energies for each size, one giving no filament breaking and one giving breaking; the dotted line is a guide to the eye). The agreement between the assumption and the results of the simulations is remarkable. The fact that our simple analytic model for the critical size slightly overestimates filament melting compared to the MD prediction for the smaller filament size (see Figure 3) can be explained by realizing that our volume calculations slightly overestimate the energy available to melt, since in the foam some recoils leave the cascade volume. Figure 3 also shows the result of the experimental irradiation of Ne into Au (described below) and the curve with the predicted critical filament size for this type of irradiation (dash line). The model clearly predicts no damage in this case, since the experimental conditions indicate a point that is well above the critical size line.

To analyze the upper critical size, we follow the evolution after irradiation of the defect clusters shown in Figure 2 and found first interstitial loops migrating to the surface of the filament, and vacancy cluster following later on, which are results that allow us to estimate the complete annihilation of vacancies and interstitials in times of the order of 1 ns. To estimate this time in a general case, Figure 4 shows migration times needed for interstitials and vacancies in Au to travel across a filament of a given diameter and annihilate at the surface. The time required for the I-loop annihilation in our MD simulation, shown in Figure 4 by a

dx.doi.org/10.1021/nl201383u |Nano Lett. 2012, 12, 3351–3355

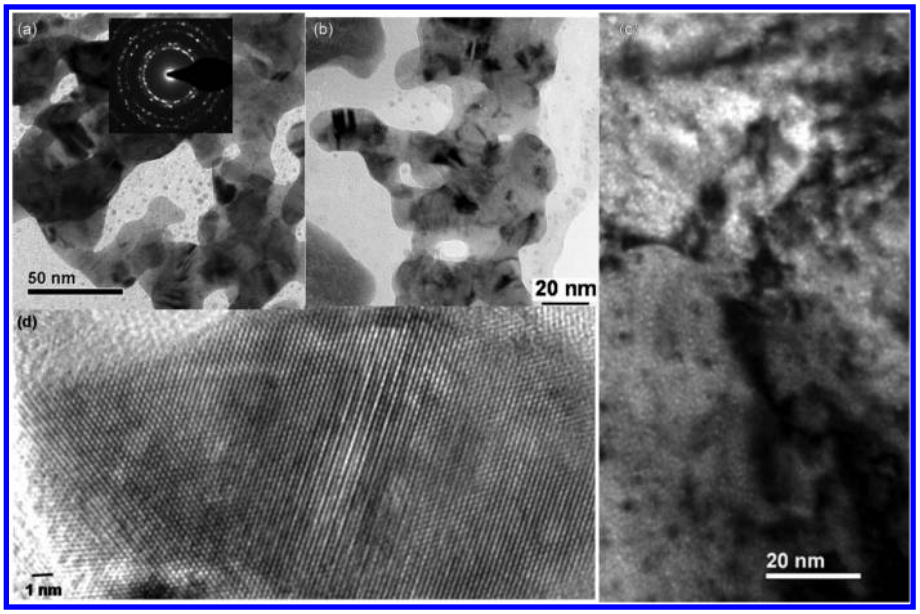

Figure 6. Irradiation of nanofoams, experimental results. Nanoporous Au irradiation at 77 K with 45 keV Ne+ to a dose of 4.5×10^{14} /cm^2 (1.5 dpa) at 300 K. (a) Unirradiated sample, including small area diffraction (SAD) pattern showing that the ligaments are polycrystalline. (b) Bright-field TEM image of np-Au after irradiation. (c) Under-focused bright-field TEM images of single crystal Au film after same irradiation conditions, showing Ne bubbles as white dots, and dislocation loops as black features. (d) High-resolution TEM image of np-Au after irradiation. Note the absence of radiation damage in (b) and (d).

square, is shorter than that suggested for interstitials in the bulk of Au implying a much greater diffusivity in filaments, likely due to the presence of a bias due to image forces created by the surface. The use of bulk diffusion parameters is then a conservative assumption for diffusion in nanoscale filaments. Diffusivity of vacancy clusters depends on cluster size, and therefore for our estimate of the window of radiation endurance reported in Figure 5 and discussed below we assume it to be a factor of 100 times smaller than the single vacancy diffusivity.

Having defined this annihilation time, damage accumulation would occur if new defects arrive before the previous ones have reached the surface, implying the existence of a dose rate thershold. At dose-rates above such threshold, the material will accumulate damage due to the formation of larger and less mobile defect cluster. Reciprocally, if the defects produced by a cascade diffuse to the surface before another cascade hits a representative volume, there will be no defect accumulation. Accelerated dynamics techniques, like parallel replica simulations,[21] might provide accurate estimates of diffusion times for large vacancy clusters, to better quantify these regimes.

To define the upper critical ligament size for foams under a given irradiation condition (irradiation conditions define the average cascade size and the time between cascades), the key issue is then to compare the time between cascades (dose-rate dependent) affecting a given representative volume (PKA energy dependent) to the time a defect cluster takes to annihilate at the surface of a ligament (ligament size and temperature dependent). The time between cascades depends on the dose-rate and on the exact value of the representative volume; to make an estimation, we take this volume as a cube of side L equal to about twice a typical cascade length scale. The horizontal lines in Figure 4 are calculated for $L = 8$ nm and three different ion dose-rates, namely 10^{13}, 10^{15}, and 10^{17} ions/cm^2/sec. Therefore, as shown in that figure, if the ligament is too large, defect migration to available surfaces would take too long, while for ligament sizes giving a diffusion time below the size limit given we expect defects would not accumulate, effectively making the foam radiation resistant. The upper critical size is then defined by the intersection of the horizontal line corresponding to the particular dose-rate of interest with the diffusion line characterizing the mobility of defects in the material.

Combining the results for the upper and lower critical size, we report in Figure 5 the window of radiation resistance in terms of ligament diameter versus dose-rate for nanofoam Au irradiated with 45 keV Ne at room temperature. We show the upper critical limit for three different diffusivities D, namely 5×10^{-9}, 5×10^{-10}, and 5×10^{-11} cm^2/sec. The lower critical limit has been determined for 15 keV cascades as created by 45 keV Ne ions into Au. A triangular window of radiation endurance is clearly predicted.

Experimental Results. We have carried out ion irradiation experiments on Au nanofoams for conditions for which the model predicts radiation resistance, as shown in Figure 5. We used Au nanofoams synthesized by electrochemically dealloying Si from evaporated amorphous Si−Au thin films.[16] During dealloying, as Si is etched away, Au atoms self-assemble in a nanocrystalline porous network. Each ligament in the honeycomb structure of the nanofoam can be seen as a nanowire. For the Au foam shown in the transmission electron microscopy (TEM) image in Figure 6, the ligament diameter was approximately 10−20 nm with a pore size of 20−50 nm, leading to an approximate density of 35−45%. The metallic foam is made of nanocrystalline grains, probably enhancing its radiation-resistant properties[7] compared to the single crystal foams considered in our simulations. These nanocrystals include pre-existing twins and stacking faults, as expected for Au, a low stacking fault fcc material. Irradiation at room temperature with 45 keV Ne ions to a dose of 4.5×10^{14}/cm^2 (dose-rate of $\sim 1 \times 10^{13}$ ions/cm^2/s or 0.033 dpa/s for a total of 1.5 dpa) generating PKAs of a maximum energy of 15 keV had little effect on the morphology

dx.doi.org/10.1021/nl201383u |*Nano Lett.* 2012, 12, 3351–3355

(e.g., coarsening and/or densification), as shown in Figure 6b,d suggesting radiation tolerance. Figure 5 shows the region in the parameter space where the experiment has been conducted, falling inside the window of radiation tolerance predicted by our model. This agreement provides support to our model because it shows that the foam structure is unaltered by an irradiation under these conditions. For comparison, Figure 6c shows significant damage accumulation in single crystal Au under the same irradiation conditions, as it is known for fcc materials irradiated up to this dose.

Summary and Conclusions. A typical dose in a nuclear reactor pressure vessel is of the order of 0.01 dpa during a lifetime of 30 years of full operation, giving a dose-rate of 1×10^{-11} dpa/sec. The fuel cladding in a Gen IV reactor is expected to receive a dose-rate of 1−5 dpa/year or $1-5 \times 10^{-9}$ dpa/sec; for fuels, this number may be orders of magnitude larger. A dose-rate of 1×10^{-9} dpa/sec represents a cascade over the representative volume every 10^3 s. This is orders of magnitude larger than the time needed for defects to diffuse out of the foam ligaments. Foams would then be extremely resistant to these environments.

Simulations performed in this work show that the properties of foams under irradiation depend on two limiting length scales, namely, (i) the size of its ligaments compared to collision cascade sizes and (ii) the distance that the defects migrate in the time interval between collision cascades.

When the ligament size is comparable to the cascade size we observe emission of planar defects (SFs and twins) and even melting and breaking of ligaments. This radiation sensitivity leads to changes in foam topology, including lowering of its surface area. Therefore, foams with ligaments comparable or smaller than cascade size are not adequate for radiation environments.

On the other hand, foams with ligament size larger than the distance defects migrate in the time interval between cascades would accumulate damage in a similar way as "bulk" material, as larger and less mobile clusters of defects are created. In between these sizes, the foam will annihilate defects at surfaces, experiencing "self-healing". This conclusion is supported by our experimental results on Au nanofoams.

Our combined experiments, simulations, and modeling results suggest then the existence of a window in the parameter space of foams under irradiation where this nanostructured materials show radiation resistance. Further investigating the radiation behavior of nanofoams has therefore high payoff potential in the search for materials with radiation endurance.

AUTHOR INFORMATION

Corresponding Author
*E-mail: caro@lanl.gov.

ACKNOWLEDGMENT

We acknowledge J. C. Thorp and J. K. Baldwin for assistance in sample synthesis at the Center for Integrated Nanotechnologies (CINT). E.M.B. acknowledges support from CONICET, PICT-2009, and a SeCTyP grant from University of Cuyo. Work at LANL was supported by the Center for Materials at Irradiation and Mechanical Extremes, an Energy Frontier Research Center funded by the U.S. Department of Energy (Award Number 2008LANL1026) at Los Alamos National Laboratory, and by CINT, a Department of Energy, Office of Basic Energy Sciences user facility. E.M.B. designed the study and the simulations and contributed to write the paper. J.D.M. performed most of the simulations. A.C. wrote the paper. A.M., M.N., S.T.P., and Y.Q.W performed the experiments (synthesized the nanofoams, carried out the irradiations, and performed TEM characterization). L.Z.R. performed some of the filament simulations. F.A. and M.D. created the numerical samples. D.F. contributed to the writing of the paper.

REFERENCES

(1) Odette, G. R.; Hoelzer, D. T. Irradiation-tolerant Nanostructured Ferritic Alloys: Transforming Helium from a Liability to an Asset. *JOM* **2010**, *62*, 84–92.

(2) Novikov, L. S.; et al. Radiation effects on spacecraft materials. *J. Surf. Invest.: X-ray, Synchrotron and Neutron Tech.* **2009**, *3*, 199–214.

(3) Zinkle, S.; Ghoniem, N. Helium-cooled refractory alloys first wall and blanket evaluation. *Fusion Eng. Des.* **2000**, *709*, 49–50.

(4) Misra, A.; Demkowicz, M. J.; Zhang, X.; Hoagland, R. G. The radiation damage tolerance of ultra-high strength nanolayered composites. *JOM* **2007**, *59*, 62–65.

(5) Demkowicz, M. J.; Hoagland, R. G.; Hirth, J. P. Interface structure and radiation damage resistance in Cu-Nb multilayer nanocomposites. *Phys. Rev. Lett.* **2008**, *100*, 136102.

(6) Samaras, M.; Derlet, P. M.; Van Swygenhoven, H.; Victoria, M. Computer simulation of displacement cascades in nanocrystalline Ni. *Phys. Rev. Lett.* **2002**, *88*, 125505.

(7) Bai, X. M.; et al. Efficient Annealing of Radiation Damage Near Grain Boundaries via Interstitial Emission. *Science* **2010**, *327*, 1631–1634.

(8) Heubeck N. B. Nuclear fuel elements made from nanophase materials. U.S. Patent 5,805,657, 1998.

(9) Erhart, P.; et al. *Phys. Rev.* **2005**, *B 72*, 052104.

(10) Biener, J.; et al. Size Effects on the Mechanical Behavior of Nanoporous Au. *Nano Lett.* **2006**, *6*, 2379–2382.

(11) Gyulassy, A. G.; et al. Topologically clean distance fields. *IEEE Trans. Visualization Comput. Graphics* **2007**, *13*, 1432–1439.

(12) Crowson, D. A.; Farkas, D.; Corcoran, S. Geometric relaxation of nanoporous metals: The role of surface relaxation. *Scr. Mater.* **2007**, *56*, 919–922.

(13) Crowson, D. A.; Farkas, D.; Corcoran, S. Mechanical stability of nanoporous metals with small ligament sizes. *Scr. Mater.* **2009**, *61*, 497–499.

(14) Foiles, S. M.; Baskes, M. I.; Daw, M. S. Embedded-atom method functions for the fcc metals Cu, Ag, Au, Ni, Pd, Pt, and their alloys. *Phys. Rev.* **1986**, *B 33*, 7983–7991.

(15) Antoniou, A.; et al. Controlled nanoporous Pt morphologies by varying deposition parameters. *Appl. Phys. Lett.* **2009**, *95*, 073116.

(16) Thorp, J. C.; et al. Formation of nanoporous noble metal thin films by electrochemical dealloying of Pt_xSi_{1-x}. *Appl. Phys. Lett.* **2006**, *88*, 033110.

(17) Li, H.; Misra, A.; Baldwin, J. K.; Picraux, S. T. Synthesis and Characterization of Nanoporous Pt-Ni Alloys. *Appl. Phys. Lett.* **2009**, *95*, 201902.

(18) Bringa, E. M.; Nordlund, K.; Keinonen, J. Cratering-energy regimes: From linear collision cascades to heat spikes to macroscopic impacts. *Phys. Rev. B* **2001**, *64*, 235426.

(19) Ziegler, J. F. SRIM - The stopping and range of ions in matter. *Nuclear Instrum. Methods Phys. Res., Sect B* **2010**, *268*, 1818–1823.

(20) Alurralde, M.; Caro, A.; Victoria, M. Radiation-damage cascades — liquid droplet treatment of subcascade interactions. *J. Nucl. Mater.* **1991**, *183*, 33–45.

(21) Voter, A. Parallel replica method for dynamics of infrequent events. *Phys. Rev. B* **1998**, *57*, 13985–13988.